



Technical Sciences  
Academy of Romania  
[www.jesi.astr.ro](http://www.jesi.astr.ro)

## **Journal of Engineering Sciences and Innovation**

Volume 9, Issue 4 / 2024, p. 431-448

<http://doi.org.10.56958/jesi.2024.9.4.431>

**F. Electrical, Electronics Engineering,  
Computer Sciences and Engineering**

*Received 24 September 2024*

*Accepted 4 December 2024*

*Received in revised form 20 November 2024*

### **Design and validation of an electrically assisted modular attachment demonstrator for lightweight cycles**

**VLAD TEODORAȘCU\*, NICOLAE BURNETE, LEVENTE BOTOND  
KOC SIS, IRINA DUMA, NICOLAE VLAD BURNETE, ANDREIA  
MOLEA, IOANA CRISTINA SECHEL, DAN MIHAI FILIMON**

*Technical University of Cluj-Napoca, Faculty of Automotive Engineering Mechatronics  
and Mechanical Engineering, Cluj-Napoca, Romania 400641*

**Abstract.** Sustainable transportation solutions are essential for enhancing resource efficiency and reducing greenhouse gas emissions. Significant contributions to this goal have been made by the cycling sector by increasing its presence in urban areas logistics. The primary means for this increase is the usage of cargo cycles. There are numerous advantages associated with it, such as: high versatility, functionality without emissions, lightweight build, and the ability to travel through areas in which conventional vehicles are prohibited. This paper reports the process of designing an experimental demonstrator for an electrically assisted attachment that can be used to convert most cycle vehicles into cargo variants. The attachment is designed to overcome one of the major drawbacks of traditional cargo cycles, namely the lack of modularity. This implies that users previously had to transport the empty cargo area even when not actively involved in delivery tasks. By removing the attachment, the user can convert the cycle for personal use. However, when required, the attachment can be added which, together with the electrical assistance system, can increase delivery efficiency. The paper aims to present the development process of the three-dimensional model of the attachment using computer-aided design techniques, highlighting the universal coupling mechanism and variable storage space. Additionally, vehicle dynamics simulations were performed to evaluate the stability of the system during operation and to ensure the validity of the proposed design.

**Keywords:** Micromobility, Green logistics, Sustainability, Cargo cycles, Electrical assistance, Green mobility, Zero emissions

---

\*Correspondence address: [Vlad.Teodorascu@campus.utcluj.ro](mailto:Vlad.Teodorascu@campus.utcluj.ro)

## 1. Introduction

In the European Union (EU) over 23% of greenhouse gas emissions have been attributed to urban transportation [1], positioning it as a critical area of focus for reducing environmental impact in cities and metropolitan areas. Urban logistics significantly contribute to the implementation of sustainable solutions by addressing challenges related to emissions, noise, and traffic congestion. The adoption of green logistics in urban settings has driven the growing demand for electric vehicles, cargo bikes, and other electric mobility options as cleaner transportation alternatives. This transition has heightened the demand for freight and passenger transport solutions that can effectively navigate the limited spaces of densely populated urban areas, utilizing micromobility options to tackle these challenges.

The adoption of light electric vehicles such as cycles (e-cycles) and their cargo variants (e-cargo cycles) has proven to be a promising solution to the urban mobility challenges. E-cargo cycles offer a balance between e-cycles and traditional vehicles regarding transport capacity, range, and cost [2]. One of the key advantages of e-cargo cycles over their non-electrified counterparts is their electric powertrain, which supports larger payload capacities, longer travel distances, and reduces driver fatigue [3]. Furthermore, e-cargo cycles do not emit local pollutants, allowing them to access city centers and other areas where cars are restricted. Given that e-cargo cycles are primarily used for delivery in urban settings, trip efficiency is a crucial metric for their effectiveness in urban logistics. This efficiency is influenced by travel distance, traffic density, and the cargo weight and volume occupied by a delivery payload. Although a higher delivery capacity generally implies greater efficiency, studies have indicated that the efficiency of e-cargo cycle delivery trips decreases as the drop size increases [4]. This translates into the fact that, anytime the cargo cycle is not used for business purposes, the trip efficiency is too low to justify the usage of such a vehicle. One measure to overcome this drawback is through the usage of cargo attachments like trailers. These micromobility solutions are widely utilized across various regions globally to expand transportation options being employed for the transportation of goods and resources in situations where other transportation methods are less cost-efficient [5]. Trailers enable up to three times the transport capacity of a regular pedal electric cycle (PEDELEC) vehicle, with weights up to 200 kg [6,7,8].

Given the rising interest for micromobility as a mean to reach green transportation, the aim of the present paper is to highlight the design of an electrically assisted cargo attachment for cycles. The attachment enables the use of all two-wheeled pedal vehicles for logistics purposes, offering the following major advantages: increased versatility, optimized transport costs, reduced energy consumption, and significantly lowered greenhouse gas emissions and congestion produced by cars and vans used for delivering goods in city centers and other densely populated areas.

The aim of the prototype is to contribute to the decarbonization of urban transport by developing a prototype of a modular electrically assisted attachment for transporting goods using pedal vehicles. Using an attachment for goods transportation is a new application area, as these are most commonly used for transporting children. Additionally, compared to current pedal vehicle cargo transport options, the proposed solution introduces three original concepts for this type of system:

- Flexibility: The ability to adapt to various types of pedal vehicles;
- Variable storage volume: To maximize transport efficiency;
- Independent electric assistance for the attachment: It does not rely on the PEDELECs' electric assist system.

Based on an examination of the existent attachment and trailer solutions [9,10,11,12] a three-dimensional model of an electrically assisted cargo attachment was designed. Computer-aided design software was used to conceptualize the attachment with a focus towards the modular cargo space and universal attachment mechanism. Furthermore, vehicle dynamics simulations were performed to evaluate whether the proposed constructive design is valid and stable during operation [13].

## **2. Design considerations of the attachment**

Two of the main features that the design must reflect are the modularity of the system and the simplicity of the mechanical components that the users will interact with. Furthermore, since the attachment will be equipped with an electrical assistance system, the weight of the electrical components such as the battery, motors and wiring must be taken into account in the overall weight of the demonstrator. These reasons impose several restrictions on the materials that can be used for the frame of the attachment.

The attachment was designed for urban applications such as delivery of parcels and products. Therefore, safety regulations and standardized vehicle dimensions are at the forefront of the design considerations. The attachment and bicycle should fit the regulations for roads meant for PEDELEC usage both in size, shape and performance. Since the attachment is meant to have a storage space with variable volume, the minimum and maximum dimensions should be compliant with public road regulations [14,15,16,17].

### *2.1.1. Compliance to legal framework*

Since all micromobility solutions are heavily reliant on urban infrastructure to fully maximize the decarbonization potential [18,19,20], compliance with safety policies is at the forefront of developing a safe and efficient mobility solution. In the case of attachments and trailers for PEDELECs, the regulatory norms are closely related to the legislation present for cycle vehicles and the usage of public roads and micromobility infrastructure [14,15,16,17].

The European standard EN 15918:2011 included in the British Standards Institution (BSI) Standards Publication Cycles — Cycle trailer — Safety requirements and test methods describes a number of requirements that the attachment must comply with. Among these, the constructive requirements include [16]:

- The height of the pitch pivot between the connecting device and the trailer shall not exceed 400 mm above a road surface for cycle trailers with a total mass exceeding 30 kg;
- The roadway and any parts of the trailer which move or rotate relative to it when the trailer is in motion, shall not be within the access zone if the trailer is meant for transporting human passengers. Nether shall there be within the access zone, any shear or compression points between moving parts that can close to less than 12 mm, except if this motion occurs only when the trailer or a part of it is being erected, folded or adjusted (e.g. adjustment of the backrest);
- The cycle trailer shall be equipped with a parking brake. The trailer shall not move more than 50 mm after the brake has been applied;
- Cycle trailers shall be designed such that a vertical obstacle cannot be caught between a wheel and the body of the cycle trailer when the cycle trailer is drawn forwards past obstacles (Fig. 1);

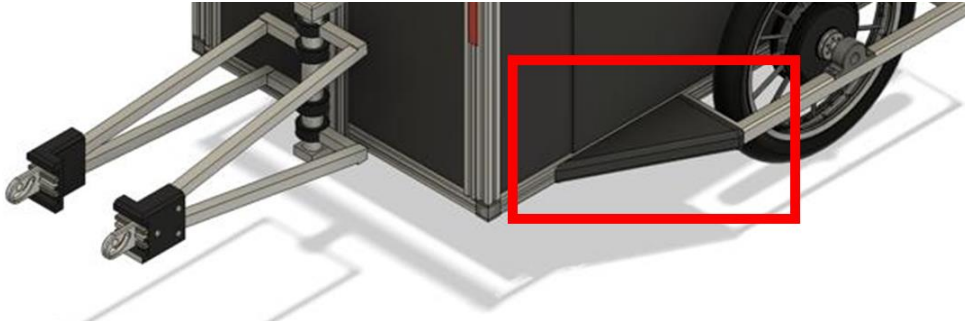


Fig. 1. Side guard equipped to avoid lateral obstacles during travelling.

- The connecting device of the cycle trailer shall allow the cycle to be turned at least  $40^\circ$  in either direction relative to the center line of the cycle trailer (Fig. 2);
- The center lines of the cycle and cycle trailer, when parallel, shall not be more than 100 mm apart (Fig. 3).

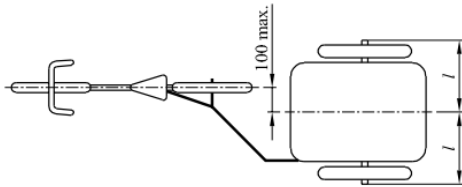


Fig. 2. Centre lines of the cycle and cycle trailer [16].

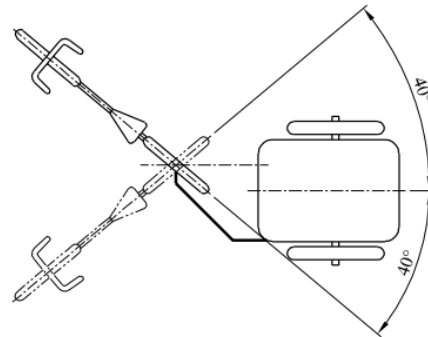


Fig. 3. Turning angle of cycle relative to the cycle trailer [16].

Similarly, the corresponding standard in the United States ASTM F1975:09 includes requirements for developing and testing Nonpowered Bicycle Trailers Designed for Human Passengers. Among these, the constructive requirements include [14,15]:

- A trailer shall be equipped with a rear reflector; side reflectors are required on wheels;
- The backrest shall have a minimum height of 350 mm, and the seated height space shall be a minimum of 550 mm.

Since urban policies are of significant importance in the process of shifting the transportation methods to more sustainable solutions, the different implementations of each country must be taken into account. One of the most significant type of regulation is the restriction of vehicle access to certain parts of the city [6,21,22,23]. In the topic of bicycle trailers, an example of national policy implementation is considered for Romania (Regulations for the Implementation of Emergency Ordinance 195/2002 Approved by Government Decision 1391/2006), where specifications include [17]:

- Article 15: A trailer attached to a bicycle must be equipped at the rear with a red fluorescent-reflective device. Additionally, if the rear light of the bicycle is obstructed by the trailer, the trailer must also be equipped with a red light;
- Article 153 (2): Bicycles can carry a light trailer with a single axle [17].

### 2.1.2. Design requirements

The initial stage of designing the attachment involves defining all the requirements that will be fulfilled by the model. Firstly, in order to ensure complete modularity in usage, the attachment must be compatible with most pedal-assisted light vehicles. Therefore, one of the main requirements that the attachment should fulfill is compatibility. Through the study of available literature and different models of both cycles and attachments on the market [24], the following options were identified:

- Attaching the trailer with a hitch onto the rear wheel Axle (Fig. 4) – The main information that the users must be aware of is the type of axle that each specific cycle has, in order to determine whether an adapter has to be used in order to attach the trailer. The identified types of axles are:
  - Quick release/skewer axle - The quick release axle has a lever that fixes the axle in place with a threaded coupling element on the opposite end;
  - Thru axle – The Thru axle is common on newer bicycles with disc brakes, electric bikes and mountain bikes;
  - Bolt-on axle – The bolt-on axle is fixed with threaded coupling elements on both sides and it is common on fixed gear and single speed bicycles, as well as internally geared hubs.
- Attaching the trailer on the seat post (Fig. 5) – This method requires the tow bar of the attachment to be fixed on the seat post of the bicycle by removing it from the main frame and threading it through a flange or clamping it directly on the post.



Fig. 4. Attachment of the trailer on the rear wheel axle [10].



Fig. 5. Attachment of the trailer on the seat post [9].

Another key requirement is the durability of the attachment. This requirement has a direct impact on the system's performance by considering the various weather and road conditions the users may encounter. This is taken into account by selecting adequate materials for the frame and cover that are both light and have optimal yield and tensile strength. Through the evaluation of existent commercial solutions, the following options were identified to be utilized most often [9,10,11,12]: aluminum, carbon fiber, synthetic fabric, steel plastic and resin.

The third requirement in close relationship with the intended design is the variable cargo space. This feature allows the user to adjust the necessary volume of the attachment in order to maximize delivery efficiency. This feature must ensure intuitiveness in the mechanical systems that the user will interact with, being at the same time safe to operate in most scenarios. Also due to the fact that the frame of

the attachment will have different dimensions based on the desired volume, ensuring that the contents are safe and secured is also mandatory at all times.

The final requirement that has been considered is the weight of the attachment. Determined by the shape, restrictions in dimensions and material selection, the weight of the attachment will have a significant impact in developing the electrical assistance system and, therefore, on the overall performance of the prototype. Furthermore, the mass limit for the transported payload for both the minimum and maximum volume of the cargo space have been considered as such:

- Minimum volume – maximum cargo mass of 150 kg;
- Maximum volume – maximum cargo mass of 200 kg.

### 2.1.3. Functional requirements

The functional requirements of the electrically assisted bicycle attachment define the essential capabilities and features that the system must possess to meet user needs and operational expectations. One of the key functional requirements is protecting the electrical components needed for the power assistance system. These include: the controllers for the electrical DC motors, battery pack, wiring, sensors and microcontrollers. All the electrical components are secured in a designated compartment located under the cargo deck and the wiring leading to the DC motors are covered on the path leading to the control unit and the battery (Fig. 6).

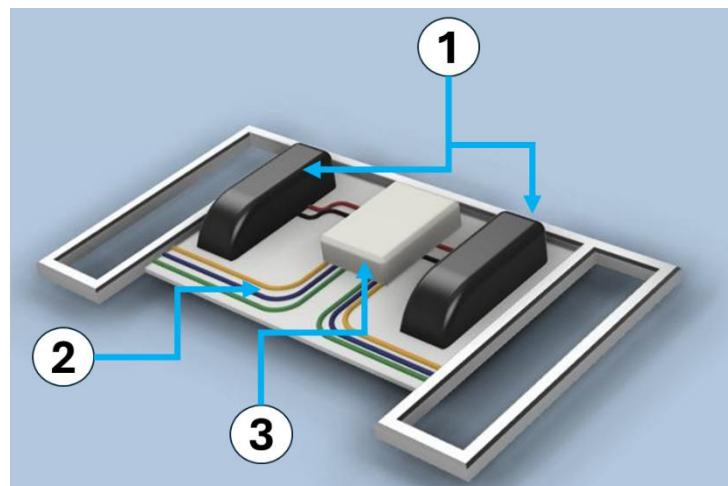


Fig. 6. Electrical components for the power assistance system:  
1) Batteries; 2) Wiring; 3) Controllers and sensors [25].

In terms of safety and road regulation, as previously mentioned, a red fluorescent-reflective device must be installed on the rear of the attachment [17]. Furthermore, the braking system of the attachment must seamlessly integrate with the bicycle's existing braking system, including regenerative braking capabilities.

Considering the aspects of safe delivery trips, the attachment must be fully equipped with the proper kit to ensure successful transportation of the load. These requirements target aspects such as:

- Water insulation of the cargo area;
- Ratchet straps to secure the cargo load in place during transportation;
- Deflection device to prevent obstacles from being lodged between the wheels and the body of the attachment [16];
- Barrier against small projectiles that might be encountered while travelling[16].

## 2.2. Three-dimensional models for the components and subsystems

The use of Computer-Aided Design (CAD) in the development of a 3D model for a prototype is a fundamental process that bridges the gap between conceptual design and physical realization [26]. CAD tools enable precise and detailed visualization, allowing designers to create, modify, and optimize models in a virtual environment before any physical production begins [27]. In order to better visualize and evaluate the attachment, computer-aided design tools have been used to first translate the identified requirements at a component level and to assemble the final version. Another important aspect of using CAD tool in the process of documenting the development of the attachment is the ability to fully define a bill of materials before moving to physical components, bringing efficiency in both costs and time.

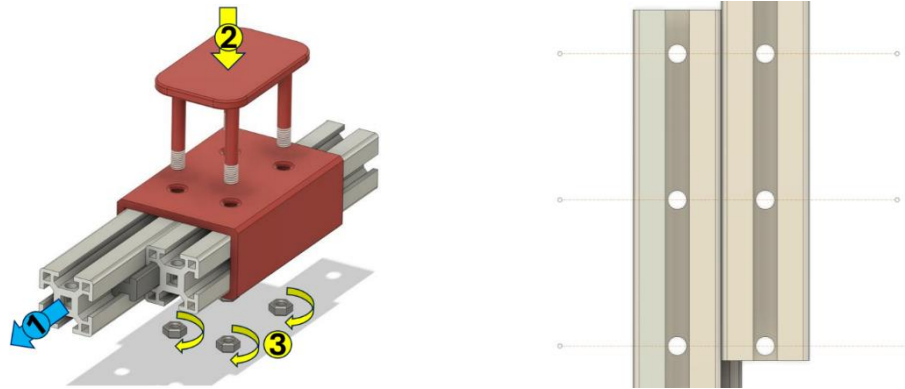
Having individual models for each component allows for a better visualization of the assembled attachment through the ability to evaluate the system in all available settings for the variable cargo space.

### 2.2.1. Design of the attachment frame

By evaluating the existent offers for commercially available solutions [9,10,11,12], the most suitable products were identified to be 30x30 mm aluminum profiles and dedicated fasteners for the connections between them.

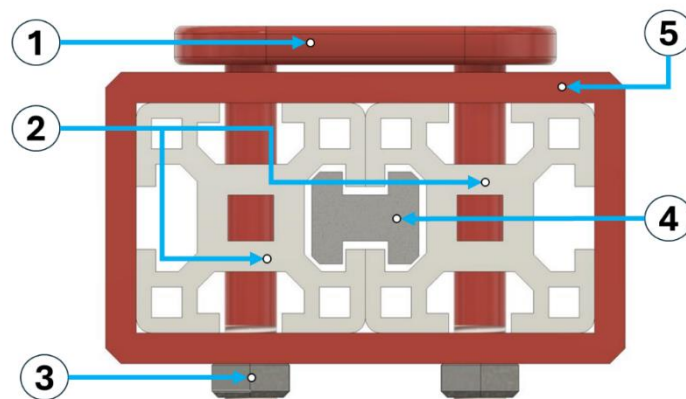
To achieve the variable storage cargo space, the attachment frame has been split into fixed and movable components. As shown in Fig. 7.b, the aluminum profiles have been provided with drilled holes that line up as the movable profile slides against the fixed one (Fig. 7.a). After the desired extension has been achieved, a plate with 4 threaded rods and fitting threaded coupling elements (Fig. 7.c), components 1 and 3) are used to fix the position of the frame (Fig. 7.a). The complete assembly of the system is shown in Fig. 7.c. As shown, the two aluminum frame components in Fig. 7.c, elements 2 slide in one direction via a central rod (Fig. 7.c, element 4) that ensures linear movement in only one direction. Furthermore, a case has been used to ensure structural stability (Fig. 7.c, element 5).





a)

b)



c)

Fig. 7. Modular system for adjusting the cargo volume: a) Adjusting and fixing the aluminum profiles in the desired position; b) Intended alignment of the aluminum profiles; c) Fixed position and assembly components.

This system is used to modify both the length and the width of the attachment independently. The cargo space specifications are:

- Length: minimum 934 mm, maximum 1334 mm;
- Height: minimum 860 mm, maximum 1355 mm.

### 2.2.2. Design of the universal coupling system

As previously mentioned, one of the main features of the attachment is the ability to be used by most models of light pedal assisted vehicles. The proposed solution

involves the usage of universal sockets for the aforementioned rear wheel cycle axles and an adjustable system for the width at which the system can be set to accommodate multiple sizes of the rear wheel hub shell.

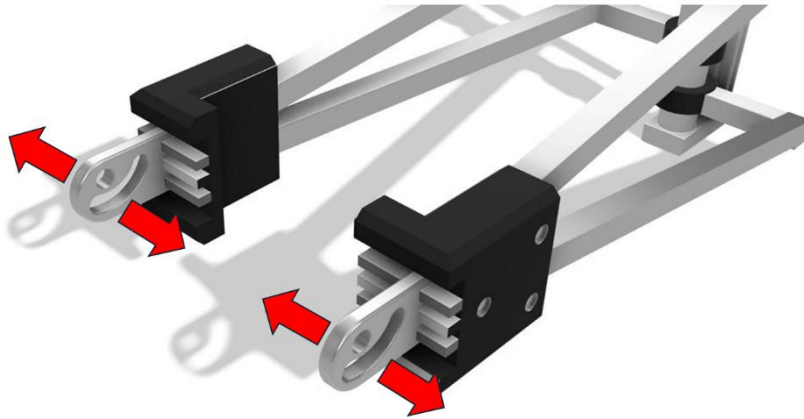


Fig. 8. Universal coupling system.

As shown in Fig. 8, the components housing the universal sockets can each slide closer or further from the center in order to be adjusted at the perfect distance to fit the rear wheel hub.

## 2.2. Vehicle dynamics calculations

Determining the optimal conditions in which the attachment can be used is essential for the validation of the proposed design. The targeted parameters of the simulations are the forces acting on the coupling element between the attachment and the cycle. Furthermore, an analysis of the maximum rollover angle for uphill and downhill conditions has been performed on possible size variations that the cargo space can support as well as multiple load weights.

Table 1. Values, Dimensions, and Description for the equation parameters [28,29,30]

| Symbol          | Description   | Value and Unit        |
|-----------------|---|-----------------------|
| A_H             | Attachment height   | 0.86 ÷ 1.35 [m]       |
| A_L             | Attachment length   | 0.93 ÷ 1.33 [m]       |
| C_L             | Coupling element length                                       | 0.65 [m]              |
| b               | Distance between rear cycle axle and centre of gravity        | 0.37 [m]              |
| b <sub>1</sub>  | Distance between attachment axle and centre of gravity        | 0.19 ÷ 0.25 [m]       |
| a               | Distance between front cycle axle and centre of gravity       | 0.59 [m]              |
| a <sub>1</sub>  | Distance between coupling element pivot and centre of gravity | 0.50 ÷ 0.84 [m]       |
| G <sub>1</sub>  | Gravitational force of the Attachment                         | 1471.50 ÷ 1962.00 [N] |
| G               | Gravitational force of the cycle-rider system                 | 931.95 [N]            |
| Mr <sub>1</sub> | Rolling resistance torque of the front wheel of the cycle     | 4976 [Nm]             |

| Symbol          | Description   | Value and Unit    |
|-----------------|---|-------------------|
| $Mr_2$          | Rolling resistance torque of the rear wheel of the cycle                  | 4976 [Nm]         |
| $Mr_3$          | Rolling resistance torque of the wheel of the attachment                  | 24655 [Nm]        |
| $Rr_1$          | Rolling resistance force of the wheel of the attachment                   | 140.33 [N]        |
| $Rr$            | Rolling resistance force of the rear wheel of the cycle                   | 88.87 [N]         |
| $Z_1$           | Normal reaction force of the road on the front cycle axle                 | 464.54 [N]        |
| $Z_2$           | Normal reaction force of the road on the rear cycle axle                  | 557.45 [N]        |
| $Z_3$           | Normal reaction force of the road on the attachment axle                  | 771.28÷1285.5 [N] |
| $\alpha$        | Road slope  | 10 [°]            |
| $A_1$           | Distance between attachment axle and cycle rear axle                      | 1.34 ÷ 1.74 [m]   |
| $A$             | Distance between rear and front cycle axles                               | 1.07 [m]          |
| $R$             | Force applied to the endpoints of the coupling element                    | 1123.6÷1872.6 [N] |
| $F_c$           | Force applied to the coupling element                                     | 255.52 [N]        |
| $F_r$           | Tractive force of the rear cycle wheel                                    | 13522 [N]         |
| $F_{r1}$        | Tractive force of the attachment wheel                                    | 74667 [N]         |
| $h_c$           | Distance between coupling element and road surface                        | 0.40 [m]          |
| $h_g$           | Distance between the centre of gravity of the cycle and road surface      | 1.14 [m]          |
| $h_{g1}$        | Distance between the centre of gravity of the attachment and road surface | 1.04 ÷ 1.11 [m]   |
| $h_a$           | Height of the cycle-rider system  | 1.75 [m]          |
| $\alpha_{Ru}$   | Maximum road slope for uphill   | 11.72÷9.52[°]     |
| $\alpha_{Rc}$   | Maximum road slope for downhill   | 48.93÷81.24[°]    |
| $\alpha_{Sl_u}$ | Highest uphill road slope value at which wheel slip can occur             | 9.46÷5.91[°]      |
| $\alpha_{Sl_c}$ | Highest downhill road slope value at which wheel slip can occur           | 17.87÷10.51[°]    |
| $\varphi$       | Road adherence coefficient considered for dry asphalt                     | 0.8 [-]           |

Specified in Table 1 are the symbols, descriptions and values for the vectors depicted in Fig. 9, as well as the parameters used in the equations (1)÷(9) [13]. Furthermore, as shown, the forces presented in Fig. 9 that act outside the system's X (longitudinal) and Y (lateral) axes defined by the road surface and a perpendicular to it, are composed from their sin and cos components (similar to gravitational forces  $G$  and  $G_1$ ).

To account for the different dimensions that the attachment can extend or compress to, several dimensions that specify the length and height of the attachment ( $A_H$ ,  $A_L$ ,  $a_1$ ,  $b_1$ ,  $A_1$  and  $h_{g1}$ ) have been considered to their minimum and maximum values, as mentioned in Table 1.

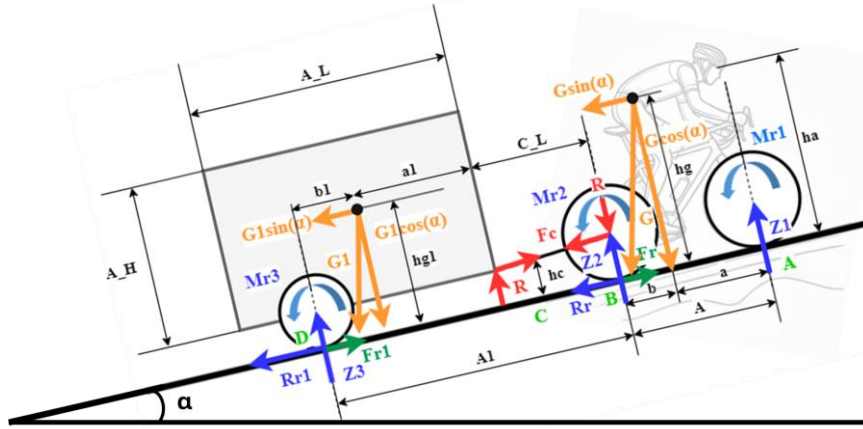


Fig. 9. Rolling resistances for the cycle-attachment system.

Determining the longitudinal stability of the system involves the calculation of the maximum road slope that the system will be able to traverse. In this sense, the maximum road slope is calculated both for uphill and downhill scenarios ( $\alpha_{Ru}$  and  $\alpha_{Rc}$ ).

- In the uphill scenario the rollover can occur around the rear axle of the cycle:

$$\alpha_{Ru} = \arctan\left(\frac{b \cdot G}{hg \cdot G + hc \cdot G_1}\right); \quad (1)$$

- In the downhill scenario the rollover can occur in the front axle of the cycle:

$$\alpha_{Rc} = \arctan\left(\frac{a \cdot G}{hg \cdot G - hc \cdot G_1}\right); \quad (2)$$

Since rollover cannot occur without the loss of traction, the highest road slope value  $\alpha$  at which wheel slip can occur can be determined as such:

- For the uphill scenario:

$$\alpha_{Sl_u} = \arctan\left(\frac{\varphi \cdot b \cdot G}{(A - hg \cdot \varphi) \cdot G + (A_1 - hc \cdot \varphi) \cdot G_1}\right); \quad (3)$$

- For the downhill scenario:

$$\alpha_{Sl_c} = \arctan\left(\frac{\varphi \cdot a \cdot G}{(A_1 - hc \cdot \varphi) \cdot G + (A - hg \cdot \varphi) \cdot G_1}\right); \quad (4)$$

To determine the equilibrium parameters of the attachment, the first component to be evaluated is the coupling element between the attachment and the cycle. The force applied to the coupling element ( $F_c$ ) can be determined using the following equations:

$$F_c = \begin{cases} G_1 & \text{if } \alpha = 0 \\ G_1 \cdot \sin(\alpha) & \text{if } \alpha \neq 0 \end{cases} \quad (5)$$

Next, to determine the force applied to the endpoints of the coupling element (R):

- The sum of torques in point D can be written as:

$$\sum (M)_D : R \cdot A_1 + hg_1 \cdot G_1 \cdot \cos(\alpha) - F_c \cdot hc = 0 \quad (6)$$

- Extracting the force applied to the endpoints of the coupling element (R):

$$R = \frac{F_c \cdot hc - hg_1 \cdot G_1 \cdot \cos(\alpha) - b_1 \cdot G_1 \cdot \sin(\alpha)}{A_1}; \quad (7)$$

To determine the normal reaction force of the road on the attachment axle ( $Z_3$ ):

- The sum of torques in point C can be written as:

$$\begin{aligned} \sum (M)_C : Z_3 \cdot A_1 - (hg_1 - hc) \cdot G_1 \cdot \sin(\alpha) - a_1 \cdot G_1 \cdot \sin(\alpha) \\ = 0 \end{aligned} \quad (8)$$

- Extracting the normal reaction force of the road on the attachment axle ( $Z_3$ ) [13]:

$$Z_3 = \frac{a_1 \cdot G_1 \cdot \cos(\alpha) + (hg_1 - hc) \cdot G_1 \cdot \sin(\alpha)}{A_1}; \quad (9)$$

### 2.3.1. Simulation parameters and results

In order to capture a comprehensive array of scenarios, the following conditions have been considered while calculating the aforementioned parameters in equations (1)÷(4), (7), (9):

- The minimum and maximum dimensions of the attachment have been considered in separate calculations;
- The mass of the payload has been incremented with a factor of 10 kg;
- The road slope has been incremented with a factor of 1°;
- The variation in distance between the centre of gravity of the cycle and road surface (hg) was evaluated for three of possible positions that the rider might be in:
  - 1143 mm – Seated position;
  - 1180 mm – Standing position;
  - 920 mm – Aerodynamic or leaning forward position [30].

An important condition for the longitudinal stability of the attachment is determining the highest road slope value  $\alpha$  at which wheel slip can occur for both uphill and downhill scenarios. The maximum angle values of  $\alpha$  for different cargo loads (G1 Table 1) and for constant friction coefficient  $\phi = 0,8$  [-] considered for a dry, asphalt road in good conditions[13] are shown in Figs. 10 and 11.

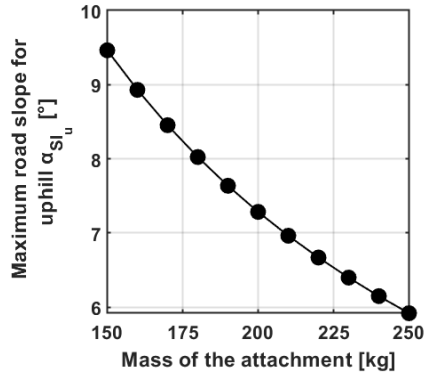


Fig. 10. The highest road slope value  $\alpha$  at which wheel slip can occur for uphill operation calculated for multiple attachment mass values.

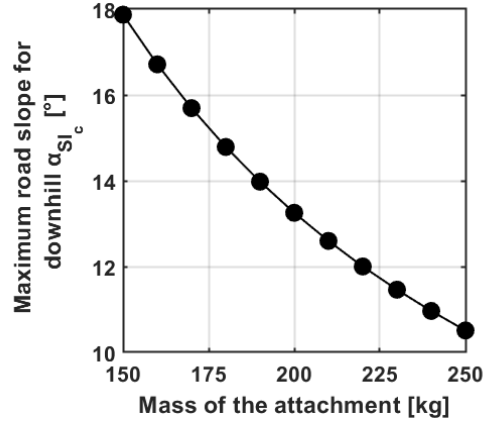


Fig. 11. The highest road slope value  $\alpha$  at which wheel slip can occur for downhill operation calculated for multiple attachment mass values.

The results shown in Figs. 10 and 11 are indicative of the fact that, as the cargo mass increases due to heavier loads, the value of the maximum angle of the road slope that the attachment can overcome without the effect of wheel slip, decreases. Similarly, the calculation of the highest road slope value  $\alpha$  at which rollover can occur for both uphill and downhill scenarios provides the following output (Fig. 12 and 13).

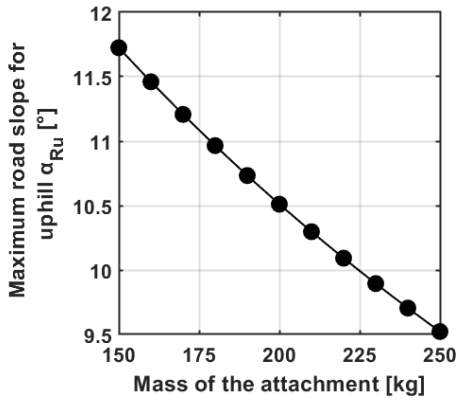


Fig. 12. The highest road slope value  $\alpha$  at which rollover can occur for uphill operation calculated for multiple attachment mass values.

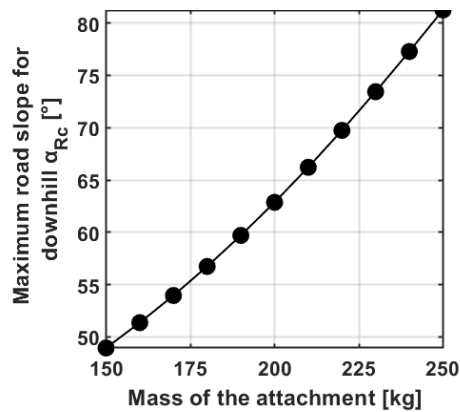


Fig. 13. The highest road slope value  $\alpha$  at which rollover can occur for downhill operation calculated for multiple attachment mass values.

As indicated by the results, the highest road slope value  $\alpha$  that the attachment can overcome without rollover for the uphill scenario, decreases as the gravitational

force of the attachment increases (G1 Table1). Conversely, for the downhill scenario the highest road slope value  $\alpha$  that the attachment can overcome without rollover increases with as the cargo load increases. This is indicative of the fact that the additional mass increases the stability of the system in downhill operation. The results also prove the longitudinal stability of the system since the highest road slope values  $\alpha$  that the attachment can overcome without rollover are higher than the road slope values calculated for the wheel slip [13].

The following results highlight two forces that act upon the attachment during uphill operation namely the force applied to the endpoints of the coupling element R and normal reaction force of the road on the attachment axle  $Z_3$ . In the first analysed scenario showcased in Fig. 14 and Fig. 15, the attachment has been evaluated for a  $10^\circ$  road slope with an increasing cargo mass (from 150 kg to 250 kg with a 10 kg increment). The output shows a linear increase in both forces as the attachment mass increases. These results provide crucial information for the design of the coupling element as well as equilibrium parameters by determining the maximum values that the attachment can handle during operation.

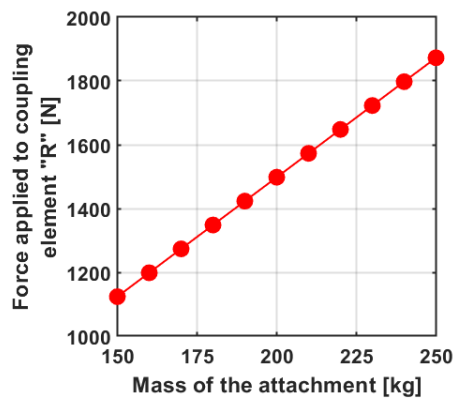


Fig. 14. Variation of the force applied to the coupling element across different attachment mass values.

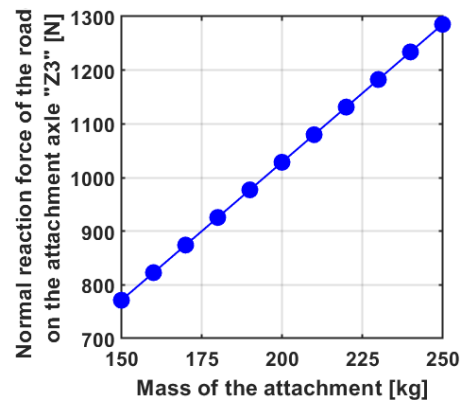


Fig. 15. Variation of the normal reaction force of the road on the attachment axle across different attachment mass values.

In the last scenario highlighted in Fig. 16 and Fig. 17 the attachment has been evaluated for multiple road slope values and a constant cargo load of 200 kg. As presented in Fig. 16, the force applied to the coupling element R decreases as the value of the road slope increases  $\alpha$ . Conversely the normal reaction force of the road applied on the attachment axle  $Z_3$  increases as the value of the road slope  $\alpha$  is incremented.

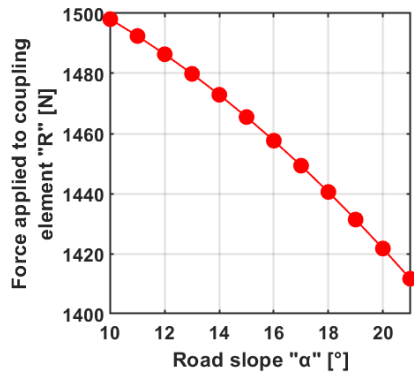


Fig. 16. Variation of the force applied to the coupling element across different road slope values for a constant attachment mass of 200kg.

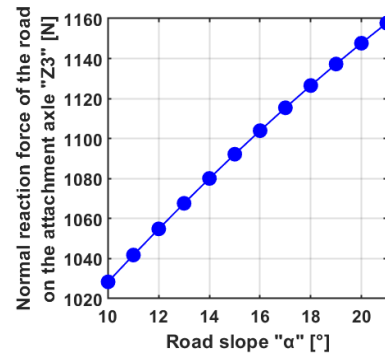


Fig. 17. Variation of the normal reaction force of the road on the attachment axle across different road slope values for a constant attachment mass of 200kg.

### 3. Results

#### 3.1. Design concept

The complete assembly of the attachment is showcased in Fig. 18 and Fig. 19. The cargo space is protected from all directions by resin panels that provide the capability of sliding when the dimensions of the frame change. To ensure complete coverage without introducing more complexity to the system, the top of the attachment can be equipped with a rain protective cover made out of synthetic outdoor fabric.



Fig. 18. Renderings for the final assembly design of the attachment in the setting for minimum height and length.

In the fully extended version (Fig. 19), the water-repellent cover can be re-attached to fit the extended dimensions. To account for the changes in dimensions, the bottom part of the cargo space is covered with panels that can be stored inside the attachment and added to fit the frame settings. Furthermore, the panels also provide cover to the space used to store the electrical components.





Fig. 19. Rendering for the final assembly design of the attachment in the setting for maximum height and length.

#### 4. Conclusions and discussions

The use of an attachment for light pedal-assisted vehicles offers benefits similar to those of a cargo cycle by providing additional cargo space and enabling the transition of logistic services to a more sustainable alternative. The proposed solution addresses the drawback of having a single-use vehicle by introducing modularity, allowing the attachment to be removed entirely for non-delivery trips. The ability to adjust the dimensions of the cargo space enhances efficiency, and by equipping the system with an electric assistance feature, users can transport larger cargo loads.

During the design process, several challenges were identified, including meeting the functional requirements while ensuring compliance with legislation and urban policies. Another crucial aspect was determining the optimal solution for the variable storage space while maintaining structural stability. The proposed solution involves predetermined settings in which the attachment frame can be fixed in, to ensure predictability in its performance during operation.

Vehicle dynamics simulations revealed the conditions under which the system can remain stable and illustrated the various physical phenomena that impact the system. The parameters for longitudinal stability were considered for both the effect of rollover and wheel slip and the analysis of the forces that act on the attachment resulted in relevant data for the equilibrium of the system.

#### 5. Acknowledgements

This work was supported by the Technical University of Cluj Napoca under the GNaC ARUT 2023 National Grant Program, grant number 25/01-07-2024.

#### References:

- [1] E. Commission, *Communication from the Commission to the European Parliament, the Council, the European economic and social committee and the committee of the regions*, Bruxelles, 2013.
- [2] Gruber J., Kihm A., Lenz B., *A new vehicle for urban freight? An ex-ante evaluation of electric cargo bikes in courier services*, *Research in Transportation Business & Management*, **11**, 2014, p. 53–62.
- [3] T. for London, *Cycle freight in London: A scoping study*, London, 2009.
- [4] Cuenot F., Fulton L., Staub J., *The prospect for modal shifts in passenger transport worldwide and impacts on energy use and CO<sub>2</sub>*, *Energy Policy*, **41**, 2012, p. 98–106.
- [5] Dorsey B., *Sustainable Intermediate Transport in West Africa: Quality Before Quantity*, *World Transport Policy & Practice*, **14**, 2, Jul. 2008.
- [6] Lenz B. and Riehle E., *Bikes for Urban Freight?*, <https://doi.org/10.3141/2379-05>, no. 2379, p. 39–45, 2013, doi: 10.3141/2379-05.

- [7] Schier M. et al., *Innovative two-wheeler technologies for future mobility concepts*, 2016 11<sup>th</sup> International Conference on Ecological Vehicles and Renewable Energies, EVER 2016, 2016.
- [8] Oyesiku O.O., Akinyemi O.O, Giwa S.O., Lawal N.S., Adetifa B.O., *Evaluation of Rural Transportation Technology: A Case Study of Bicycle and Motorcycle Trailers*, Jurnal Kejuruteraan, **31**, 1, Apr. 2019, p. 11–18, doi: 10.17576/jkukm-2019-31(1)-02.
- [9] Burley, Travoy® Cargo Trailer -. Accessed: Aug. 13, 2024. [Online]. Available: <https://burley.com/en-in/products/travoy>
- [10] Burley, Flatbed™ Cargo Trailer. Accessed: Aug. 13, 2024. [Online]. Available: <https://burley.com/en-in/products/flatbed>
- [11] TAXXI, LOAD Heavy - trailer for heavy loads and luggage. Accessed: Aug. 13, 2024. [Online]. Available: <https://mytaxxi.de/en/products/taxxi-load-heavy>
- [12] Wike, Aluminum Landscaping & Utility Cargo Bike Trailer. Accessed: Aug. 13, 2024. [Online]. Available: <https://wikeinc.com/en-ca/products/cargo-landscaping-trailer>
- [13] A. ; C. N. ; B. I. Todoruţ, *Elemente de dinamica autovehiculelor*, Cluj-Napoca, U.T.PRESS, 2021.
- [14] ASTM F2917-12, *Standard Specification for Bicycle Trailer Cycles Designed for Human Passengers*, 2012, ASTM International. doi: 10.1520/F2917-12R18.
- [15] ASTM F1975-09, *Standard Specification for Nonpowered Bicycle Trailers Designed for Human Passengers*, 2015, ASTM INTERNATIONAL. doi: 10.1520/F1975-09.
- [16] BS EN 15918:2011, ‘Cycles — Cycle trailer — Safety requirements and test methods,’ 2011.
- [17] DECISION No. 1,391 of October 4, 2006 (updated) for the approval of the Regulation for the implementation of Government Emergency Ordinance No. 195/2002 regarding traffic on public roads. Art. 153(2), Art. 15. Gov, 2006.
- [18] Faxér A.Y., Olausson E., Olsson L., Smith G., Pettersson S., *Electric cargo bike with a twist - A field test of two innovative bicycle concepts*, in 31<sup>st</sup> International Electric Vehicle Symposium and Exhibition, EVS 2018 and International Electric Vehicle Technology Conference 2018, EVTeC 2018.
- [19] Rudolph C. and Gruber J., *Cargo cycles in commercial transport: Potentials, constraints, and recommendations*, Research in Transportation Business and Management, **24**, 2017.
- [20] Schliwa G., Armitage R., Aziz S., Evans S., Rhoades J., *Sustainable city logistics - Making cargo cycles viable for urban freight transport*, Research in Transportation Business and Management, **15**, 2015.
- [21] Narayanan S. and Antoniou C., *Electric cargo cycles - A comprehensive review*, Transp. Policy (Oxf), **116**, 2022.
- [22] Navarro C., Roca-Riu M., Furió S., Estrada M., *Designing New Models for Energy Efficiency in Urban Freight Transport for Smart Cities and its Application to the Spanish Case*, Transportation Research Procedia, 2016.
- [23] Choubassi C., Seedah D.P.K., Jiang N., Walton C.M., *Economic Analysis of Cargo Cycles for Urban Mail Delivery*, <https://doi.org/10.3141/2547-14>, **2547**, p. 102–110, 2016.
- [24] Bini R.R., Dagnese F., Kleinpaul J., *Bicycle types and sizes*, Biomechanics of Cycling, 9783319055398, Feb. 2014, p. 63–69.
- [25] Dora R. and Mulla G.B., *Materials for e-bike and end to end design aspects*, Materials Today: Proceedings, Elsevier Ltd, p. 1374–1380, 2023.
- [26] Berretti S., Werghi N., Del Bimbo A., Pala P., *Matching 3D face scans using interest points and local histogram descriptors*, Comput Graph, **37**, 5, 2013, p. 509–525.
- [27] Veltkamp R.C. et al., SHREC’11 track: 3D face models retrieval, Eurographics Workshop on 3D Object Retrieval, EG 3DOR, p. 89–95, 2011.
- [28] Alam F., Khan I., Chowdhury H., Alam F., Khan I., AN EXPERIMENTAL STUDY OF BICYCLEAERODYNAMICS, 2011.
- [29] Baldissera P. and Delprete C., *Rolling resistance, vertical load and optimal number of wheels in human-powered vehicle design*, Proc Inst Mech Eng P J Sport Eng Technol, **231**, 1, 2017, p. 33–42.
- [30] D. Gordon. Wilson, *Bicycling Science*, fourth edition, 2020, Accessed: Aug. 13, 2024. [Online]. Available: [https://books.google.com/books/about/Bicycling\\_Science\\_fourth\\_edition.html?id=wCngDwAAQBAJ](https://books.google.com/books/about/Bicycling_Science_fourth_edition.html?id=wCngDwAAQBAJ)